# Soil Moisture Retrieval in the Heihe River Basin Based on the Real Thermal Inertia Method

Chunfeng Ma, Weizhen Wang, Xujun Han, and Xin Li

***Abstract*—Remotely sensed thermal inertia method has been recognized as a promising approach for land surface soil moisture retrieval from the early 1970's. In order to estimate the land surface soil moisture in arid regions, a real thermal inertia (RTI) model was formulated based on the heat conduction equation and an approximated energy budget equation at the land surface using the land surface temperature and reflectance measured by Moderate Resolution Imaging Spectroradiometer (MODIS). The soil thermal inertia of Heihe River Basin (HRB) was retrieved based on the RTI model. Furthermore, using a thermal inertia-soil moisture model along with auxiliary data such as soil texture and bulk density, land surface soil moisture was estimated. The results were verified experimentally using the observations made at three automatic weather stations (AWS). The coefficient of the correlation between the retrieved values of soil thermal inertia and measured ones was with above $R = 0.6$ and the root mean square error of soil moisture was 0.072 $m^3m^{-3}$. The soil moisture in the HRB exhibits a seasonal variation with higher values in summer and autumn and lower values in winter and spring, and also exhibits considerable spatial variation with higher values in the upstream district and lower values in the downstream district.**

***Index Terms*—Heihe river basin, real thermal inertia model, remote sensing, soil moisture.**

## I. Introduction

### A. Background

THE soil moisture is an important hydrological state variable which plays a key role in understanding the land surface water and energy budgets [1]–[5]. As the second largest inland river basin in China [6]–[8], the Heihe River Basin (HRB) is located in the northwest of China, the water scarcity [9]–[12] is an obstacle to the social development of the region. The upstream district of the HRB is one of the major pastoral areas of Qinghai Province. The mid-reaches district of the HRB, in which the Zhangye oasis is located, is an important area for food production and a zone for demonstrating High-tech Agriculture [13]. Since the annual rainfall of this district is less than 200 mm, most of the crop water requirements are supplied by irrigation from the Heihe River. Therefore, it is of major significance to understand the behavior of soil moisture in the HRB and to estimate the soil moisture variability in the district.

The thermal inertia method has been shown to be a promising approach [14] for land surface soil moisture retrieval from the early 1970's [15]–[19]. Many studies have been conducted to develop the model to obtain thermal inertia from remotely sensed data. Watson *et al.* (1971; 1974) [15], [16] developed a thermal inertia model for geological mapping using infrared data. Kahle *et al.* (1976) [20] obtained the first thermal inertia image using visible and infrared data, then Kahle (1977) [18] improved the early thermal inertia models using the finite difference technique. Price (1983; 1985) [21], [22] introduced the so-called apparent thermal inertia (ATI) model. Because the ATI model estimates the relative value of the real thermal inertia (RTI) and also because of its simplicity, the ATI model is often used instead of RTI model. Although the ATI presents the relative value of thermal inertia, it cannot be a full substitute for the real thermal inertia and it does not meet the requirements of precise soil moisture retrieval [23], [24], especially for agricultural landscapes [22].

A large number of soil thermal inertia-soil moisture (STI-SM) relationship models were developed [25], [26]. Pratt & Ellyett (1979) [27] calculated soil thermal inertia using the model of soil thermal conductivity and volumetric heat capacity by de Vries (1963) [28]. Price (1980) [29] extended his previous work (1977) [19] and estimated soil moisture using an empirical linear equation, but the equation parameters were valid only for the soil studied. Ma & Xue (1990) [30] reported a relationship between the soil thermal inertia and the water content (denoted MX model hereafter). Murray & Verhoef (2007) [31] adopted the concept of normalized thermal conductivity [32], [33] and developed amore mechanistic model to estimate the soil thermal inertia (MV model hereafter). Sen Lu (2009) [14] proposed a new model (denoted Lu model hereafter), which expresses the soil thermal inertia as a function of water content, based on the MV model and Sen Lu (2007) [34].

### B. Objectives

Some questions will be explored in this paper: (1) which thermal inertia model is more suitable for soil moisture retrieval in the HRB, the RTI model or the ATI model? (2) how the thermal inertia and soil moisture vary as the seasons progresses?

Manuscript received September 28, 2012; revised January 31, 2013; accepted March 02, 2013. Date of publication March 29, 2013; date of current version June 17, 2013. This paper is supported by two project groups titled "Remote Sensing Data Products in the Heihe River Basin: Algorithm Development, Data Products Generation and Application Experiments" (Grant number: KZCX2-XB3-15) and "Heihe Watershed Allied Telemetry Experimental Research" (Grant numbers: 91125001 and 91125002) which are funded by the Chinese Academy of Sciences and the National Natural Science Foundation of China, respectively. *(Corresponding author: W. Z. Wang.)*

C. F. Ma is with the Cold and Arid Regions Environmental and Engineering Research Institute, Chinese Academy of Sciences, Lanzhou 73000, China. He is also with the University of Chinese Academy of Sciences, Beijing 100049, China.

W. Z. Wang, X. J. Han, and X. Li are with the Cold and Arid Regions Environmental and Engineering Research Institute, Chinese Academy of Sciences, Lanzhou 73000, China.

Color versions of one or more of the figures in this paper are available online at http://ieeexplore.ieee.org.

Digital Object Identifier 10.1109/JSTARS.2013.2252149

And (3) how the thermal inertia and soil moisture distribute in the HRB?

The objectives of this paper are to address these questions; those are, (1) to obtain the formula of the ATI and RTI models from the heat conduction equation; (2) to compare the advantages of the ATI and the RTI models in soil moisture retrieval; (3) to analyze temporal-spatial variations of the soil thermal inertia and soil moisture in the HRB.

Firstly, the RTI model used in this analysis is obtained from the heat conduction equation and explained briefly in Section II-A. Secondly, the Lu model is introduced in Section II-B to relate the soil moisture to the thermal inertia. In Section III, The automatic weather station (AWS) data, the soil texture data and the MODIS products are described. Results are analyzed in Section IV and the conclusions and discussions of this paper are given in Section V.

## II. Models and Methods

### A. Real Thermal Inertia Model

Soil thermal inertia, $P$ $(\mathrm{Jm^{-2}K^{-1}s^{-(1/2)}})$ describes the impedance of soil to temperature variations [35], which has a strong positive correlation with soil moisture. It is defined as follows:

$$P = \sqrt{k\rho c} \tag{1}$$

where $k$ $(\mathrm{Wm^{-1}K^{-1}})$, $\rho$ $(\mathrm{kgm^{-3}})$, $c$ $(\mathrm{Jkg^{-1}K^{-1}})$ represent the soil thermal conductivity, soil density, specific heat, respectively. The thermal inertia of soil cannot be measured by a remote sensing technique directly, and hence a remotely sensed thermal inertia model is required for estimating thermal inertia [36], [37].

To establish the remotely sensed thermal inertia model, the heat conduction equation must be solved. One dimensional heat conduction equation is formulated by:

$$\frac{\partial T(z,t)}{\partial t} = \frac{k}{c\rho}\frac{\partial^2 T(z,t)}{\partial z^2} \tag{2}$$

where $T$ (K) is the soil temperature, $t$ (s) is the time, $z$ (m) is the soil depth (positive downward).A simple sinusoidal solution of (2) under the boundary conditions,

$$T(0,t) = T_m + T_0\cos(\omega t) \tag{3}$$

$$T(\infty,t) = T_m \tag{3a}$$

can be written as:

$$T(z,t) = T_m + T_0 e^{\left(-\frac{z}{D}\right)}\cos\left(\omega t - \frac{z}{D}\right) \tag{4}$$

where $T_{\mathrm{m}}$ is mean temperature, $T_0$ is amplitude of temperature variation at the soil surface. Here, $D$ is called the damping depth and is related to the thermal properties of soil and $\omega = 2\pi/t_p$ is the angular frequency $(\mathrm{s^{-1}})$ and $t_p$ is the time period of one cycle (s). As we are interested in the diurnal variation of soil temperature, It can be assumed that during the course of a day, approximately the same amount of heat $Q$ flows into the ground through the soil surface during a half day and flows out of the ground during another half of the day. We can calculate $Q$ as follows:

$$Q = k\int_{t_{\frac{p}{2}}}^{t_p}\frac{\partial T(z,t)}{\partial z}\Bigg]_{Z=0} dt = \sqrt{\frac{2}{\omega}}T_0 P \tag{5}$$

It is seen that the thermal inertia is a measure of the response of a material to temperature changes. In general, materials with high thermal inertia have more uniform surface temperature throughout the day and night than materials of low thermal inertia.

The energy budget at the soil surface can be expressed as:

$$-k\frac{\partial T(z,t)}{\partial z}\Bigg]_{z=0} = (1-\alpha)S_0 C_\tau\cos Z + \varepsilon L^{\downarrow} - L^{\uparrow} - H - E \tag{6}$$

where $\alpha$ is the shortwave albedo and $S_0$ is the solar constant; $C_\tau$ is the transmissivity of the atmosphere ($C_\tau = 0.76$ in this paper); $Z$ is the zenith angle of the sun; $\varepsilon$ is the emissivity of the surface; $L^{\downarrow}$ is the downward long wave radiation and $L^{\uparrow}$ is the upward long wave radiation; $H$ is the upward sensible heat flux and $E$ is the upward latent heat flux. Pratt *et al.* (1980) [38] proposed a simplified expression of the budget equation as follows.

$$-k\frac{\partial T(z,t)}{\partial z}\bigg|_{z=0} = (1-\alpha)S_0 C_\tau\cos Z - [A_c + B\,(T(0,t) - T_m)] \tag{7}$$

where $A_{\mathrm{c}}$ and $B$ are parameters related to the conditions above and below the soil surface.

Here we define a new function $\varphi(z,t)$ as;

$$\varphi(z,t) = (T(z,t) - T_m) - \frac{k}{B}\frac{\partial T(z,t)}{\partial z} \tag{8}$$

Hence from (7) we obtain:

$$\varphi(0,t) = -\frac{A_c}{B} + \frac{(1-\alpha)S_0 C_\tau\cos Z}{B} \tag{9}$$

Since $\varphi(0,t)$ is a periodic function of angular frequency $\omega$ if $\cos Z$ can be approximated by $A_1\cos(\omega t)$,where $A_1$ is a kind of Fourier transform coefficient and obtained as

$$A_1 = \frac{2}{t_p}\int_{-t_p/2}^{\frac{t_p}{2}}\cos Z\ cos(\omega t)dt \tag{10}$$

then (7) can be integrated to be (Carlaw, 1959) [39]

$$T(0,t) - T_m = -\frac{A_c}{B}(1-\alpha)\left\{S_0 C_\tau\frac{A_1\cos(\omega t)}{\sqrt{B^2 + \omega P^2 + \sqrt{2\omega}BP}}\right\}^{-1} \tag{11}$$

Therefore, if daily maximum temperature $T_{\max}$ occurs at $t_{\max}$, and daily minimum temperature $T_{\min}$ occurs at $t_{\min}$; and

since $\cos(\omega t_{\max}) = 1$ and $(\omega t_{\min}) = -1$, it can be obtained from

$$\frac{(1-\alpha)}{\Delta T} = \frac{1}{2S_0 C_\tau A_1}\sqrt{B^2 + \omega P^2 + \sqrt{2\omega}BP} \tag{12}$$

where $\Delta T = T_{\max} - T_{\min}$. The left hand side of (12) is called the apparent thermal inertia (ATI).

Setting

$$a = \sqrt{B^2 + \omega P^2 + \sqrt{2\omega}BP} \tag{13}$$

Solving (13) for $P$, we have

$$P = \frac{-B + \sqrt{2a^2 - B^2}}{\sqrt{2\omega}} \tag{14}$$

where parameter $B$ was introduced in (7) as an empirical constant ($\mathrm{B} = 9.6558\ \mathrm{Wm^{-1}K^{-1}}$, for water body); and parameter $\alpha$, $\Delta T$ and $A_1$ will be calculated in Section II-C.

### B. Soil Thermal Inertia-Soil Moisture Model

The high positive correlation between the soil thermal inertia and the soil moisture indicates that the soil moisture can be estimated from the soil thermal inertia [40]–[43]. However, so far, there is no general physical-based model to depict the relationship between the soil thermal inertia and the soil moisture. Lu (2009) [14] proposed a general method for soil moisture estimation from thermal inertia. In this method, the soil thermal inertia is assumed to be expressed by:

$$P = P_{dry} + (P_{sat} - P_{dry})K_p \tag{15}$$

where $P_{dry}$ and $P_{sat}$ represent the thermal inertia corresponding to dry and saturated soil conditions, respectively. $K_\mathrm{p}$ is the Kersten function [32]–[34], [44].Hereafter $P, P_{\mathrm{dry}}, P_{\mathrm{sat}}$ are expressed in $\mathrm{kJm^{-2}K^{-1}s^{-(1/2)}}$

$P_{dry}$ can be calculated from the soil porosity $(n)$ according to the following empirical equation [14], [31]:

$$P_{dry} = -1.0624n + 1.0108 \tag{16}$$

However, $P_{sat}$ depends largely upon the soil moisture, soil texture and soil bulk density, so it can be calculated by:

$$P_{sat} = \sqrt{k_{sat}C_{sat}} \tag{17}$$

where $k_{\mathrm{sat}}$ and $C_{\mathrm{sat}}$ are the soil heat conductivity and soil volumetric heat capacity corresponding to saturated soil conditions, respectively. They can be computed by the following equations:

$$k_{sat} = \left(k_{qa}^q k_o^{1-q}\right)^{1-n} k_w^n \tag{18}$$

$$C_{sat} = \rho_b c_s + \rho_w c_w n \tag{19}$$

where $k_{qa}(= 7.7\ \mathrm{Wm^{-1}K^{-1}})$ and $k_{\mathrm{w}}(= 0.594\ \mathrm{Wm^{-1}K^{-1}})$ are the conductivity of quartz and water, respectively, and $k_{\mathrm{o}}(\mathrm{Wm^{-1}K^{-1}})$ is conductivity of other mineral except for quartz. The quartz content of total solids $(q)$ is taken as the fraction of sand [31], [45] and $k_{\mathrm{o}}$ is taken as 2.0 $\mathrm{Wm^{-1}K^{-1}}$ for soils with $q > 0.2$, and 3.0 $\mathrm{Wm^{-1}K^{-1}}$ for soils with $q <= 0.2$ [32], $\rho_{\mathrm{b}}$ $(\mathrm{kgm^{-3}})$ and $\rho_{\mathrm{w}}(= 1000\ \mathrm{kgm^{-3}})$ are the soil bulk density and water density, respectively, $c_{\mathrm{s}}$ $(= 0.8\ \mathrm{kJkg^{-1}K^{-1}}$, in accordance with Ren *et al.* (2003) [46]) and $c_{\mathrm{w}}$ represent the specific heat of soil solids and water, respectively.

TABLE I
VALUES OF $\varepsilon$ AND $\mu$

| Parameters | Values | Conditions |
|---|---|---|
| $\varepsilon$ | 1.78 | 0.8<$q$<1.0 |
| | 3.84 | 0.4<$q$<=0.8 |
| | 0.93 | 0<$q$<=0.4 |
| $\mu$ | 2.0 | 0.8<$q$<1.0 |
| | 4.0 | 0.4<$q$<=0.8 |
| | 1.5 | 0<$q$<=0.4 |

According to the soil shrinkage curve model [47], the $K_{\mathrm{p}}$ function can be expressed by:

$$K_p = \exp\left[\epsilon\left(1 - S_r^{-\mu}\right)\right] \tag{20}$$

where $S_{\mathrm{r}}$ is the saturation degree of soil moisture, $\varepsilon$ and $\mu$ are the two parameters controlling function shapes and they can be determined by the sand content of soil as shown in Table I.

By inserting $\mathrm{S}_r = \theta/n$ in (20), and rearranging, the soil moisture is expressed as:

$$\theta = n\left(1 - \frac{lnK_p}{\varepsilon}\right)^{\frac{-1}{\mu}} \tag{21}$$

where $\theta$ is the soil water content and $n$ is the soil porosity.

### C. Calculation and Verification Methods

As has been described in (12), the shortwave albedo $\alpha$ and the maximum temperature difference $\Delta T$ are two key parameters of the real thermal inertia model. They should be calculated correctly.

Liang (2001) [48] developed the narrowband to broadband albedo conversion formulae for a series of sensors based on extensive radiative transfer simulations. Their formula to calculate the shortwave albedo based on the MODIS reflectance is:

$$\alpha = 0.160\alpha_1 + 0.291\alpha_2 + 0.243\alpha_3 + 0.116\alpha_4 + 0.112\alpha_5 + 0.081\alpha_7 - 0.0015 \tag{22}$$

where $\alpha_i$ $(i = 1, 2, 3, 4, 5, 7)$ represent the reflectance of different MODIS spectral bands. Liang *et al.* (2003) [49] validated this formula and found an RSE of 0.018 and $\mathrm{R}^2$ of 0.855.

The temperature difference, $\boldsymbol{\Delta T}$ can be directly derived from thermal infrared observations. In this paper, MODIS land surface temperatures were used to compute $\Delta T$ [50]:

$$\Delta T = \frac{2\left(T(t_1) - T(t_2)\right)}{\sin\left(\frac{\pi t_1}{12} + \varpi\right) - \sin\left(\frac{\pi t_2}{12} + \varpi\right)} \tag{23}$$

where, $T(t_1)$ and $T(t_2)$ represent the land surface temperature at time $t_1$ and $t_2$ at which the satellites passed, respectively. $\varpi$ is the function of geographic latitude $\varphi$ and solar declination $\delta$, formulated as:

$$\varpi = \cos^{-1}(-\tan\varphi \times \tan\delta) \tag{24}$$

$A_1$ describes the amplitude of variation in net solar radiation which land surface receives during the course of a day. It can be computed from (10), in which the cosine function of solar zenith angle, cosZ is expressed by:

$$\cos Z = \cos\delta\cos\varphi\cos\omega t + \sin\delta\sin\varphi \tag{25}$$

The definition of the thermal inertia was used to verify the performance of the real thermal inertia model. First of all, the soil conductivity and soil volumetric heat capacity were estimated from (26) [14], [28] and (27) [51], [52] using the AWS data and soil texture data:

$$k = -G\Big/\frac{\partial T}{\partial z} \tag{26}$$

$$C_v = \rho_b c_s + \theta c_w \rho_w \tag{27}$$

where $G$ $(\mathrm{Wm}^{-2})$ is the soil heat flux measured at 5 cm depth (positive downward); $\theta$ is the measured land surface soil moisture; the gradient of soil temperature was replaced by the average gradient between the surface and 10 cm depth. The later was measured directly and the former was calculated by [53], [54]:

$$T_s = \left(\frac{L^{\uparrow} - (1-\varepsilon_g)L^{\downarrow}}{\varepsilon_g \sigma}\right)^{\frac{1}{4}} \tag{28}$$

where the surface emissivity $\varepsilon_g$ was assumed to be 0.95 for bare soil surfaces and 0.98 for vegetated surfaces, and the Stefan-Boltzmann constant $\sigma = 5.67 \times 10^{-8}\ \mathrm{Wm}^{-2} \cdot \mathrm{K}^{-4}$.

Combining (1) with (26) and (27), we can get the soil thermal inertia at the AWS with which the remotely sensed retrieved soil thermal inertia can be verified. The remotely sensed soil moisture can be verified by comparing to the soil moisture measured at the stations.

## III. Data Descriptions

In this paper, three types of data, the MODIS data, the AWS data and the soil property data, were used. MODIS land surface temperature (M*D11A2) and MODIS Land Surface Reflectance (M*D09A1) products were used to drive the real thermal inertia model.

During the period of Water Allied Telemetry Experimental Research (WATER) [6], more than ten key stations were operated in the up and middle stream districts of the HRB for the ground data collection. Three of the automatic weather stations were selected in this paper as the typical ground surface types. These stations are Arou freeze/thaw observation station (Arou), (located in 38.05° N, 100.45° E, grassland surface with loam soil), Yingke oasis station (YK), (located in 38.86° N, 100.41° E, cropland surface with clay loam soil) and Huazhaizi desert station (HZZ), (located in 38.77° N, 100.31° E, desert steppe surface with sand soil). The observation parameters are the net radiation, the soil heat flux (5,15 cm), the soil moisture (10,20 cm),and the soil temperature (10,20 cm). The sensors and sampling frequency were described elsewhere [6]. All the data were collected, analyzed, and quality-examined and published by the Environmental and Ecological Science Data Centre for West China (EESDWC) [55], [56].

In addition, the Harmonized World Soil Database (vision 1.1 published by FAO and IIASA at March 26th, 2009) soil texture dataset of the HRB was used for operating the Soil Thermal Inertia-Soil Moisture model.

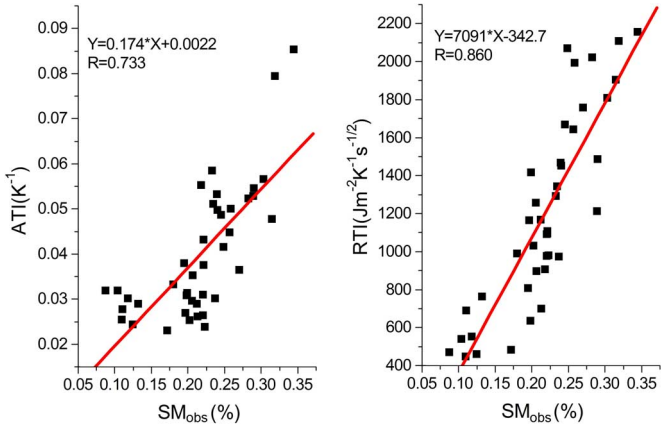


Fig. 1. Scatter plots for the soil moisture and ATI (left), and RTI (right).

## IV. Results and Discussion

### A. Comparison of ATI and RTI

Price (1985) [22] pointed out that the ATI was potentially misleading in agricultural areas and it should not be used in regions having variability in surface moisture. In order to confirm this conclusion, the soil moisture data observed at Yingke station were selected to make a comparison between the ATI and RTI. Fig. 1 shows the scatter plots for the soil moisture and the ATI, and for the RTI. The correlation coefficient $R$ for the former was 0.733 and that for the latter was 0.860. This result illustrates that RTI is better than ATI for the soil moisture retrieval in agricultural areas.

### B. Spatial-Temporal Characteristics of Soil Thermal Inertia

Fig. 2 depicts the correlation between the thermal inertia retrieved and the ground truth. The information from the figure indicates that the correlation between the values retrieved and measured at Arou station (Fig. 2(a)) was the highest and that at Yingke (Fig. 2(c)) station was the lowest. The cause of higher dispersion at Yingke station is probably abrupt changes in soil moisture in the farmland due to irrigation. However, the correlation coefficients at the three stations were larger than 0.6, which suggests that the RTI method meets the requirement of soil moisture estimation in HRB.

Fig. 3 shows abrupt changes in soil thermal inertia throughout HRB. As regards seasonal change, soil was much wetter in summer and autumn than in winter and spring, which caused higher soil thermal inertia in summer than in winter. With respect to local change, the variation of soil thermal inertia

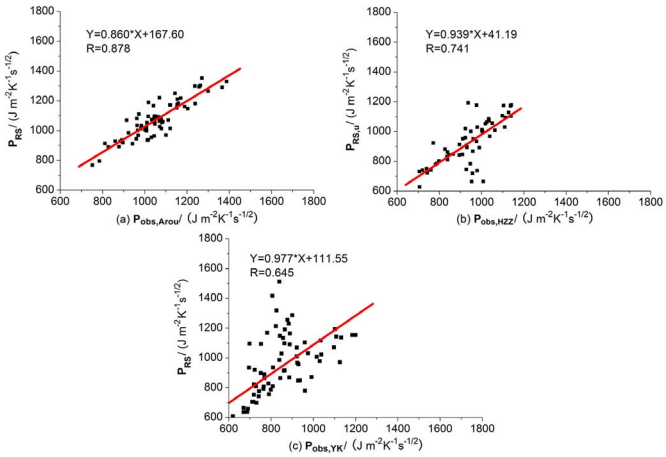


Fig. 2. Scatter plots for the soil thermal inertia retrieved and measured at three stations. (a) $\mathrm{P_{obs,Arou}/(Jm^{-2}K^{-1}s^{-1/2})}$; (b) $\mathrm{P_{obs,HZZ}/(Jm^{-2}K^{-1}s^{-1/2})}$; (c) $\mathrm{P_{obs,YK}/(Jm^{-2}K^{-1}s^{-1/2})}$.

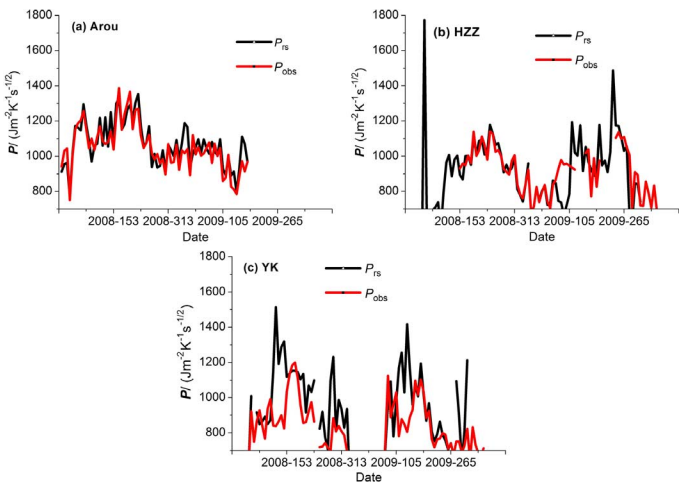


Fig. 3. Time series of the soil thermal inertia.

at Arou (Fig. 3(a)) and HZZ (Fig. 3(b)) was smaller than Yingke (Fig. 3(c)) because the land surface type of Yingke is farmland where soil moisture and cover type vary strikingly. Furthermore, farmland was irrigated during the crop growing season, which induced large changes in the soil moisture and hence soil thermal inertia.

In addition to the significant seasonal variations, the soil thermal inertia varies strikingly in space. As can be observed in Fig. 4, the soil thermal inertia in the HRB shows the pattern of high values in the up and middle stream districts and low values in the downstream district. Fig. 4(a) is the spatial distribution of the soil thermal inertia on April 4th, 2008. From the figure, it can be seen that the value of the soil thermal inertia at the upstream district and middle stream district ranged from 800 $\mathrm{Jm^{-2}K^{-1}s^{-1/2}}$ to 2000 $\mathrm{Jm^{-2}K^{-1}s^{-1/2}}$, which were larger than that at the downstream district where the values were 400–900 $\mathrm{Jm^{-2}K^{-1}s^{-1/2}}$. There are several possible reasons for these distribution characteristics: 1) higher precipitation in the upstream district results in the wetter soils, 2) permafrost in the up steam district thaws in spring, 3) uneven distribution of rocks with larger thermal inertia. Comparing Fig. 4(a) to

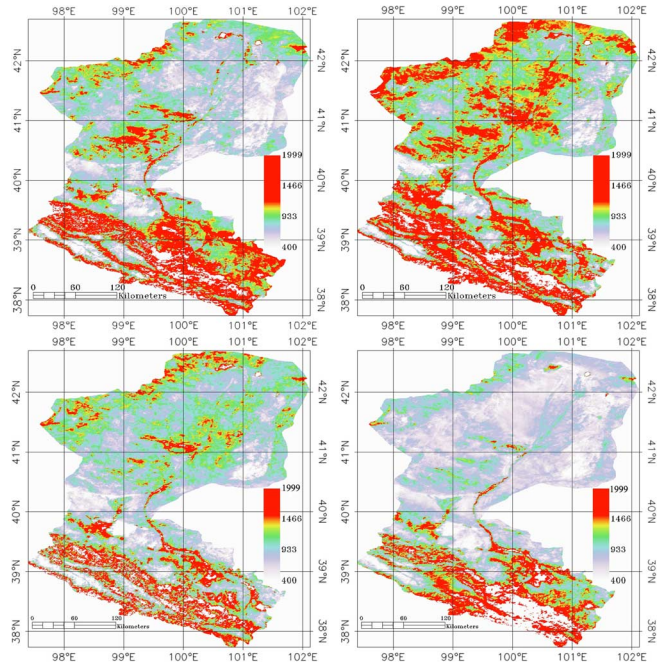


Fig. 4. Spatial distributions of soil thermal inertia at different times of year. (a) April 6th, 2008; (b) May 16th, 2008; (c) July 1st, 2008; (d) August 24th, 2008.

Fig. 4(b), we see that the soil thermal inertia in mid-May increased extremely in the mid-stream and downstream districts due to the irrigation of oasis farmland during the period of crop emergence at early in May. Fig. 4(c) and Fig. 4(d) shows the soil thermal inertia at early in July and the end of August, respectively, when the soil thermal inertia in the downstream showed a significant decrease. The reason for this decrease seems to be the intensive solar radiation and high temperature in summer. Although, summer is the rainy season in these districts, rainfall cannot compensate the large amount of evaporation which causes a serious decrease in the soil moisture.

### C. *Spatial-Temporal Characteristic of Soil Moisture*

Fig. 5 shows the seasonal variation in the soil moisture at distribution the three sites. The soil moisture was higher in summer and autumn and lower in spring and winter. The trends of retrieved values $(SM_{\mathrm{rs}})$ agree well with those of observed values $(SM_{\mathrm{obs}})$. The root mean square errors (RMSE) of the retrieved soil moisture were 0.057, 0.071 and 0,072 $\mathrm{m^3m^{-3}}$ for Arou, HZZ and Yingke, respectively. The soil moisture at Arou station is influenced by freezing/thawing processes and at Yingke was influenced by the irrigation. Soil salinization influenced the observation precision of Time Domain Reflectometer (TDR) at HZZ station, which resulted in the mismatching between the soil moisture value retrieved and observed.

Fig. 6(a) shows the spatial distribution of the soil moisture in the HRB early in June of 2008. As regards the distribution of the soil moisture, soil was much wetter in upstream and mid-stream than in downstream. By comparing Fig. 6(a) and Fig. 6(b), it is not difficult to find that the soil became drier during the period from early in June to the end of July. This significant difference results from decreased soil water due to evaporation. Additionally, a large amount of water in Heihe River was consumed

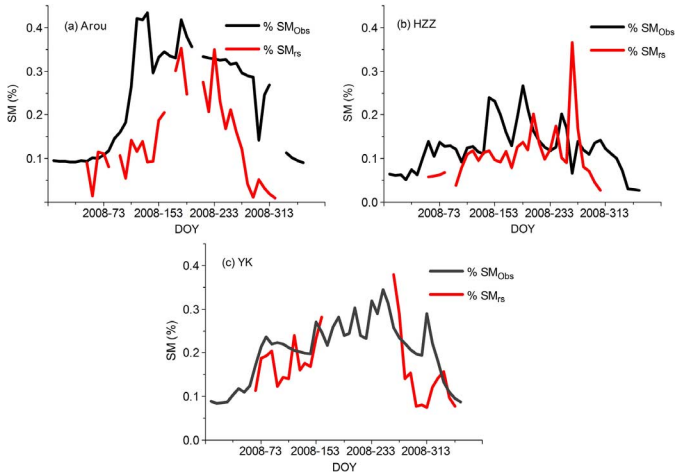


Fig. 5. Seasonal variation in soil moisture at sites.

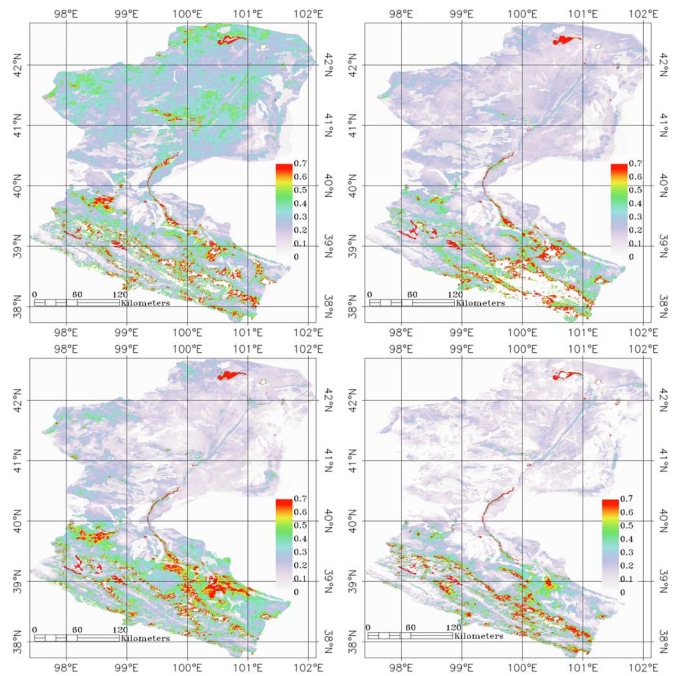


Fig. 6. Spatial distribution of soil moisture at different times of year. (a) June 1st, 2008; (b) Jul. 27th, 2008; (c) Sep. 29th, 2008; (d) Oct. 15th, 2008.

as irrigation water and diverted to the oases in mid-stream district, resulting in the water shortage to the downstream district. Fig. 6(c) and Fig. 6(d) respectively show the soil moisture at end of the September and mid-October. On the whole, the soil moisture is larger in the upstream and mid-stream districts than that in the downstream.

## V. Conclusions

The soil moisture distribution in the HRB was retrieved on the basis of remotely sensed soil thermal inertia. In this process, the soil texture and bulk density were used as the auxiliary data to operate the soil thermal inertia-soil moisture model. The retrieved results were validated against observations and the following conclusions were obtained:

A. By comparison of the performance of the ATI and RTI models in soil moisture estimation at Yingke station, the RTI model was more reliable than the ATI model to retrieve the soil moisture in the agricultural area. The RTI model was selected to retrieve the soil thermal inertia and it was convinced to give reasonable results. The coefficient of the correlation between the soil thermal inertia retrieved by remote sense and the measurements was larger than 0.6.

B. A physically-based soil thermal inertia-soil moisture model was shown to be effective to estimate soil moisture. The root mean square error of soil moisture retrieval was less 0.072 $\mathrm{m^3 m^{-3}}$.

C. The spatial-temporal analysis of the soil thermal inertia and soil moisture indicated the strong heterogeneity in the HRB due to natural complexity of the environment.

Although a few conclusions were drawn from this work, there are some deficiencies in this study. The retrieved soil thermal inertia and soil moisture values were not fully consistent with the observed ones. By analyzing both data and the methods, we can find the following reasons: i) no discrimination between bare soil and vegetated surfaces, the research region in this paper is covered by bare soil, grassland, forests, cropland, snow, and so on. So it is of significance to distinguish different land cover types. ii) Limitations of pixel scale values being validated by site observations, when we validate the retrieved values which represents a pixel scale of one square kilometers using station observations which represents point scale of less than one square meter, the scale effect cannot be ignored. To overcome the shortcoming above, a more profound work needs to be done in the future. A proposed future work could be as follows: First, physically-based thermal inertia model considering vegetated and bare soil separately should be conducted to improve the performance of soil moisture estimation in vegetated regions. Second, estimate the reflectance of brightness temperature of soil and vegetation by radiative transfer model and combine them with remotely sensed observation. Then construct a cost function and minimized it. That is, using the idea of data assimilation to promote the precision of soil moisture estimation.

## Acknowledgment

The authors wish to express heartfelt thanks to Prof. T. Kobayashi of CAREERI, who read and corrected this manuscript.

## References

[1] R. Jin and X. Li, "Improving the estimation of hydrothermal state variables in the active layer of frozen ground by assimilating in situ observations and SSM/I data," *Sci. China Series D-Earth Sci.*, vol. 52, pp. 1732–1745, Nov. 2009.

[2] N. N. Das and B. P. Mohanty, "Root zone soil moisture assessment using remote sensing and vadose zone modeling," *Vadose Zone J.*, vol. 5, pp. 296–307, Feb. 2006.

[3] R. K. Munro, W. F. Lyons, Y. Shao, M. S. Wood, L. M. Hood, and L. M. Leslie, "Modelling land surface-atmosphere interactions over the Australian continent with an emphasis on the role of soil moisture," *Environ. Model. Softw.*, vol. 13, pp. 333–339, 1998.

[4] Y.-A. Liou, S. F. Liu, and W. J. Wang, "Retrieving soil moisture from simulated brightness temperatures by a neural network," *IEEE Trans. Geosci. Remote Sens.*, vol. 39, no. 8, pp. 1662–1673, 2001, 10.1109/36.942544.

[5] S.-F. Liu, Y.-A. Liou, W.-J. Wang, J.-P. Wigneron, and J.-B. Lee, "Retrieval of crop biomass and soil moisture from measured 1.4 and 10.65 GHz brightness temperatures," *IEEE Trans. Geosci. Remote Sens.*, vol. 40, no. 6, pp. 1260–1268, Jun. 2002.

[6] X. Li, X. W. Li, Z. Y. Li, M. G. Ma, J. Wang, Q. Xiao, Q. Liu, T. Che, E. X. Chen, G. J. Yan, Z. Y. Hu, L. X. Zhang, R. Z. Chu, P. X. Su, Q. H. Liu, S. M. Liu, J. D. Wang, Z. Niu, Y. Chen, R. Jin, W. Z. Wang, Y. H. Ran, X. Z. Xin, and H. Z. Ren, "Watershed allied telemetry experimental research," *J. Geophys. Res. Atmosph.*, vol. 114, no. D22103, Sep. 2009, 10.1029/2008JD011590.

[7] Q. B. Zhang, Z. S. Li, P. X. Liu, and S. C. Xiao, "On the vulnerability of oasis forest to changing environmental conditions: Perspectives from tree rings," *Landscape Ecol.*, vol. 27, no. 3, pp. 343–353, Mar. 2012, 10.1007/s10980-011-9685-0.

[8] Z. L. Li, Z. G. Xu, Q. X. Shao, and J. Yang, "Parameter estimation and uncertainty analysis of SWAT model in upper reaches of the Heihe river basin," *Hydrolog. Process.*, vol. 23, no. 19, pp. 2744–2753, Sep. 2009, 10.1002/hyp.7371.

[9] Z. Zeng, J. Liu, P. H. Koeneman, E. Zarate, and A. Y. Hoekstra, "Assessing water footprint at river basin level: A case study for the Heihe river basin in Northwest China," *Hydrol. Earth Syst. Sci.*, vol. 16, no. 8, pp. 2771–2781, Aug. 2012, 10.5194/hess-16-2771-2012.

[10] Y. B. Wang, P. T. Wu, X. N. Zhao, and J. M. Jin, "Division of the water-saving crop planning system in the Heihe river basin," *African J. Biotechnol.*, vol. 9, pp. 9108–9117, Dec. 2010.

[11] B. Liu, W. Z. Zhao, X. X. Chang, S. B. Li, Z. H. Zhang, and M. W. Du, "Water requirements and stability of oasis ecosystem in arid region, China," *Environ. Earth Sci.*, vol. 59, no. 6, pp. 1235–1244, Jan. 2010, 10.1007/s12665-009-0112-7.

[12] Y. Wang, H. L. Xiao, and R. F. Wang, "Water scarcity and water use in economic systems in Zhangye City, Northwestern China," *Water Res. Manag.*, vol. 23, no. 13, pp. 2655–2668, Oct. 2009, 10.1007/s11269-009-9401-x.

[13] C. L. Fang, J. C. Huang, and Y. S. Liu, "Thoughts on constructing the demonstrating areas of the ecological rebuilding and economic sustainable development in Hexi region," *Chin. Geograph. Sci.*, vol. 12, no. 1, pp. 14–22, Mar. 2002.

[14] S. Lu, Z. Q. Ju, T. S. Ren, and R. Horton, "A general approach to estimate soil water content from thermal inertia," *Agricult. Forest Meteorol.*, vol. 149, pp. 1693–1698, Oct. 2009.

[15] K. Watson, L. C. Rowan, and T. W. Offield, "Application of thermal modeling in the geologic interpretation of IR images," *Remote Sen. Environ*, vol. 3, pp. 2017–2041, 1971.

[16] K. Watson and H. A. Pohn, "Thermal inertia mapping from satellites discrimination of geologic units in Oman," *J. Res. Geolog. Surv.*, vol. 2, pp. 147–158, 1974.

[17] G. A. R. Kahle, A. B. Goetz, and A. F. H. *et al.*, "Thermal inertia mapping," in *Proc. 10th Int. Symp. Remote Sensing Environ.*, 1975, vol. 2, pp. 985–994.

[18] A. B. Kahle, "A simple thermal model of the earth's surface for geologic mapping by remote sensing," *J. Geophy. Res.*, vol. 82, pp. 1673–1680, 1977.

[19] J. C. Price, "Thermal inertia mapping: A new view of the earth," *J. Geophys. Res.*, vol. 82, pp. 2582–2590, 1977.

[20] A. B. Kahle, A. R. Gillespie, and A. F. H. Goetz, "Thermal inertia imaging—New geologic mapping tool," *Geophys. Res. Lett.*, vol. 3, pp. 26–28, 1976.

[21] J. C. Price, "Estimating surface temperatures from satellite thermal infrared data—A simple formulation for the atmospheric effect," *Remote Sens. Environ.*, vol. 13, pp. 353–361, 1983.

[22] J. C. Price, "On the analysis of thermal infrared imagery—The limited utility of apparent thermal inertia," *Remote Sens. Environ.*, vol. 18, pp. 59–73, 1985.

[23] R. H. Zhang*, Experimental Remote Sensing Model and Its' Field Basis*. Beijing, China: Science Press, 1996.

[24] R. H. Zhang, "Advanced thermal inertia model and remote sensing soil moisture," (in Chinese) *Geograp. Res.*, vol. 9, pp. 101–112, 1990.

[25] T. Y. Chang, Y. C. Wang, C. C. Feng, A. D. Ziegler, T. W. Giambelluca, and Y. A. Liou, "Estimation of root zone soil moisture using apparent thermal inertia with MODIS imagery over a tropical catchment in Northern Thailand," *IEEE J. Sel. Topics Appl. Earth Observ. Remote Sens.*, vol. 5, pp. 752–761, Jun. 2012.

[26] M. Minacapilli, M. Iovino, and F. Blanda, "High resolution remote estimation of soil surface water content by a thermal inertia approach," *J. Hydrol.*, vol. 379, no. 3–4, pp. 229–238, Dec. 2009, 10.1016/j.jhydrol.2009.09.055.

[27] D. A. Pratt and C. D. Ellyett, "The thermal inertia approach to mapping of soil moisture and geology," *Remote Sens. Environ*, vol. 8, pp. 151–168, 1979.

[28] D. A. de Vries, "Thermal properties of soils," in *Physics of Plant Environment*, W. R. Van Wijk, Ed. , Amsterdam: North-Holland Publishing Company, 1963, pp. 210–235.

[29] J. C. Price, "The potential of remotely sensed thermal infrared data to infer surface soil-moisture and evaporation," *Water Resources Res.*, vol. 16, pp. 787–795, 1980.

[30] A. N. Ma and Y. Xue, "A study of remote sensing information model of soil moisture," in *Proc. 11th Asian Conf. Remote Sensing*, Beijing, 1990, pp. P-11-1–P-11-5.

[31] T. Murray and A. Verhoef, "Moving towards a more mechanistic approach in the determination of soil heat flux from remote measurements—II. Diurnal shape of soil heat flux," *Agricult. Forest Meteorol.*, vol. 147, no. 1–2, pp. 88–97, Nov. 2007, 10.1016/j.agrformet.2007.06.009.

[32] O. Johansen, "Thermal Conductivity of Soils," Ph.D. dissertation, Trondheim, Norway, 1975.

[33] J. Cote and J. M. Konrad, "A generalized thermal conductivity model for soils and construction materials," *Can. Geotech. J.*, vol. 42, pp. 443–458, Apr. 2005.

[34] S. Lu, T. S. Ren, Y. S. Gong, and R. Horton, "An improved model for predicting soil thermal conductivity from water content at room temperature," *Soil Sci. Soc. Amer. J.*, vol. 71, no. 1, pp. 8–14, Jan.–Feb. 2007, 10.2136/sssaj2006.0041.

[35] M. Minacapilli, C. Cammalleri, G. Ciraolo, F. D'Asaro, M. Iovino, and A. Maltese, "Thermal inertia modeling for soil surface water content estimation: A laboratory experiment," *Soil Sci. Soc. Amer. J.*, vol. 76, no. 1, pp. 92–100, Jan. 2012, 10.2136/sssaj2011.0122.

[36] Z. H. Liu and Y. Zhao, "Study on top layers soil moisture inversion using remote sensing thermal inertia method," *Sci. China Ser., D Earth Sci.*, vol. 136, pp. 552–558, 2006.

[37] P. Nasipuri, T. J. Majumdar, and D. S. Mitra, "Study of high-resolution thermal inertia over western India oil fields using ASTER data," *Acta Astronautica*, vol. 58, no. 5, pp. 270–278, Mar. 2006, 10.1016/j.actaastro.2005.11.002.

[38] D. A. Pratt, S. J. Foster, and C. D. Ellyett, "A calibration procedure for Fourier-series thermal inertia models," *Photogrammetric Eng. Remote Sens.*, vol. 46, pp. 529–538, 1980.

[39] H. S. Caralaw*, Conduction of Heat in Solids*. London: Oxford, 1959, vol. 2.7.

[40] Y.-A. Liou and A. W. England, "A land surface process radio brightness model with coupled heat and moisture transport in soil," *IEEE Trans. Geosci. Remote Sens.*, vol. 36, no. 1, pp. 273–286, 1998a.

[41] X. M. Li, A. Liu, and S. Zhang, "Use of thermal inertia approach in the monitoring of drought by remote wensing," (in Chinese) *Agricult. Res. Arid Areas*, vol. 23, pp. 54–59, 2005.

[42] Y. Cheng, "The Soil Moisture Detection for Different Vegetation Coverage Based on the MODIS Data and the Influence Analysis of the Thermal Radiant Directionality," Master's thesis, GUCAS, GUCAS, Beijing, USA, 2006.

[43] G. Y. Cai, "MODIS Data Based Thermal Inertia and Land Surface Temperature Modeling and Their Applications in Determination of Soil Moisture and Heat Exchange," Ph.D. dissertation, GUCAS, Beijing, China, 2005.

[44] Muffay and A. Verhoef, "Moving towards a more mechanistic approach in the determination of soil heat flux from remote measurements—I. A universal approach to calculate thermal inertia," *Agricult. Forest Meteorol.*, vol. 147, no. 1–2, pp. 80–87, Nov. 2007.

[45] C. D. Peters-Lidard, E. Blackburn, X. Liang, and E. F. Wood, "The effect of soil thermal conductivity parameterization on surface energy fluxes and temperatures," *J. Atmosph. Sci.*, vol. 55, no. 7, pp. 1209–1224, Apr. 1998, 10.1175/1520-0469(1998)055<1209:TEOSTC>2.0.CO;2.

[46] T. Ren, T. E. Ochsner, R. Horton, and Z. Ju, "Heat-pulse method for soil water content measurement: Influence of the specific heat of the soil solids," *Soil Sci. Soc. Amer. J.*, vol. 67, no. 6, pp. 1631–1634, Nov. –Dec. 2003, 10.2136/sssaj2003.1631.

[47] P. H. Groenevelt and C. D. Grant, "Analysis of soil shrinkage data," *Soil Tillage Res.*, vol. 79, no. 1, pp. 71–77, Sep. 2004, 10.1016/j.still.2004.03.011.

[48] S. L. Liang, "Narrowband to broadband conversions of land surface albedo I Algorithms," *Remote Sens. Environ.*, vol. 76, no. 2, pp. 213–238, May 2001.

[49] S. L. Liang, C. J. Shuey, A. L. Russ, H. L. Fang, M. Z. Chen, C. L. Walthall, C. S. T. Daughtry, and R. Hunt, "Narrowband to broadband conversions of land surface albedo: II. Validation," *Remote Sens. Environ.*, vol. 84, no. 1, pp. 25–41, Jan. 2003, 10.1016/S0034-4257(02)00068-8.

[50] J. M. Liu, Y. G. Ding, and J. J. Wang, "Experiment for estimating daly range of surface temperature over a region using AVHRR data at arbitrary time," (in Chinese) *J. Nanjing Inst. Meteorol.*, vol. 24, pp. 323–329, 2001.
[51] S. Wang, Q. ZHANG, and H. Zhang, "Characteristics of surface albedo and soil heat conductivity in sparse vegetation site," (in Chinese) *J. Desert Res.*, vol. 28, pp. 119–124, 2008.
[52] Q. Zhang, S. Wang, and G. A. Wei, "A study on parameterization of local land-surface physical processes on the Gobi of Northwest China," (in Chinese) *Chin. J. Geophys.*, vol. 46, pp. 616–623, 2003.
[53] K. Yang and J. Wang, "A temperature prediction-correction method for estimating surface soil heat flux from soil temperature and moisture data," *Sci. China Ser. D-Earth Sci.*, vol. 51, no. 5, pp. 721–729, May 2008.
[54] M. Fuchs, "Canopy thermal infrared observations," *Remote Sens. Rev.*, vol. 5, no. 1, pp. 323–333, Jan. 1990, 10.1080/02757259009532139.
[55] X. Li, Z. T. Nan, G. D. Cheng, Y. J. Ding, L. Z. Wu, L. X. Wang, J. Wang, Y. H. Ran, H. X. Li, X. D. Pan, and Z. M. Zhu, "Toward an improved data stewardship and service for environmental and ecological science data in West China," *Int. J. Digital Earth*, vol. 4, pp. 347–359, 2011.
[56] X. Li, X. W. Li, K. Roth, M. Menenti, and W. Wagner, ""Observing and modeling the catchment scale water cycle" Preface," *Hydrol. Earth System Sci.*, vol. 15, pp. 597–601, 2011.

**Chunfeng Ma** received the B.Sc. degree in Geo-Information Science and technology from the China University of Geosciences, China, in 2007 and the M.S. degree in Cartography and Geography Information System from Graduate University of Chinese Academy of Sciences (University of Chinese Academy of Sciences), Beijing, China, in 2012. He is currently working toward the Ph.D. degree at University of Chinese Academy of Sciences with the major of cartography and geography information system.

His research interests include land data assimilation land surface process simulation and soil moisture remote sensing.

**Weizhen Wang** received the Ph.D. degree from Kyushu University, Japan, in 2004.

He is working as a Professor in Cold and Cold and Arid Regions Environmental and Engineering Research Institute, Chinese Academy of Sciences, Beijing, China. His research interests include Meteorological Environmental Hydrology and Quantitative Remote Sensing of the arid regions.

**Xujun Han** received the Ph.D. degree in Cartography and Geography Information System from Graduate University of Chinese Academy of Sciences, Beijing, China, in 2008.

He is currently an Associate Professor at Cold and Arid Regions Environmental and Engineering Research Institute, Chinese Academy of Sciences. His primary research interests include land data assimilation, hydrological Remote Sensing and agricultural irrigation optimization.

**Xin Li** received the B.Sc. degree from the Nanjing University, Nanjing, China, in 1992 and the Ph.D. degree from Chinese Academy of Sciences, Beijing, China, in 1998.

He is currently a Professor at Cold and Arid Regions Environmental and Engineering Research Institute, Chinese Academy of Sciences. His primary research interests include land data assimilation, application of remote sensing and GIS in hydrology and cryosphere science, and integrated watershed modeling.